Correction

Correction: Protein phosphatase 1 regulatory subunit 1A regulates cell cycle progression in Ewing sarcoma

Wen Luo[1,2], Changxin Xu[3], Sarah Phillips[4], Aliza Gardenswartz[1], Jeremy M. Rosenblum[1], Janet Ayello[1], Stephen L. Lessnick[5], Huai-Xiang Hao[6] and Mitchell S. Cairo[1,2,4,7,8]

[1]Department of Pediatrics, New York Medical College, Valhalla, NY, USA

[2]Department of Pathology, New York Medical College, Valhalla, NY, USA

[3]James J. Peters Veterans Affairs Medical Center, Bronx, NY, USA

[4]Department of Medicine, New York Medical College, Valhalla, NY, USA

[5]Nationwide Children's Hospital, Columbus, OH, USA

[6]Novartis Institutes for BioMedical Research, Cambridge, MA, USA

[7]Department of Immunology and Microbiology, New York Medical College, Valhalla, NY, USA

[8]Department of Cell Biology and Anatomy, New York Medical College, Valhalla, NY, USA

Published:

This article has been corrected: In Figure 2C, the Western blot images for RA1 protein in A673 and EWS502 cells (the first and third images in the 'RA1' row), are accidental duplicates. The authors replaced the incorrect RA1/EWS502 image. There are also partial duplicates in the first, second, and third images of the 'tubulin' row. The authors also replaced the incorrect image for Tubulin in TC71 cells. In Figure 4, the image of wound healing assay in A673 cells at day 3 (Figure 4A) was accidentally used again to represent results in TC71 cells at day 3; the authors replaced this image with the correct wound healing image in TC71 cells at day 3. The first image in the 'D3' row In Figure 4A is an accidental duplicate of the first image in the 'D3' row of Figure 4B. One more duplication was found and corrected In Figure 5A, where CNT mice at day 28 (the second mouse image in the 'D28' row) also incorrectly represented AEW mice at day 28 (the twelfth mouse in the same row) and was replaced with the image of correct AEW mice. The corrected Figures 2, 4 and 5, produced using the original data, are shown below. The authors declare that these corrections do not change the results or conclusions of this paper.

Original article: Oncotarget. 2020; 11:1691–1704. https://doi.org/10.18632/oncotarget.27571

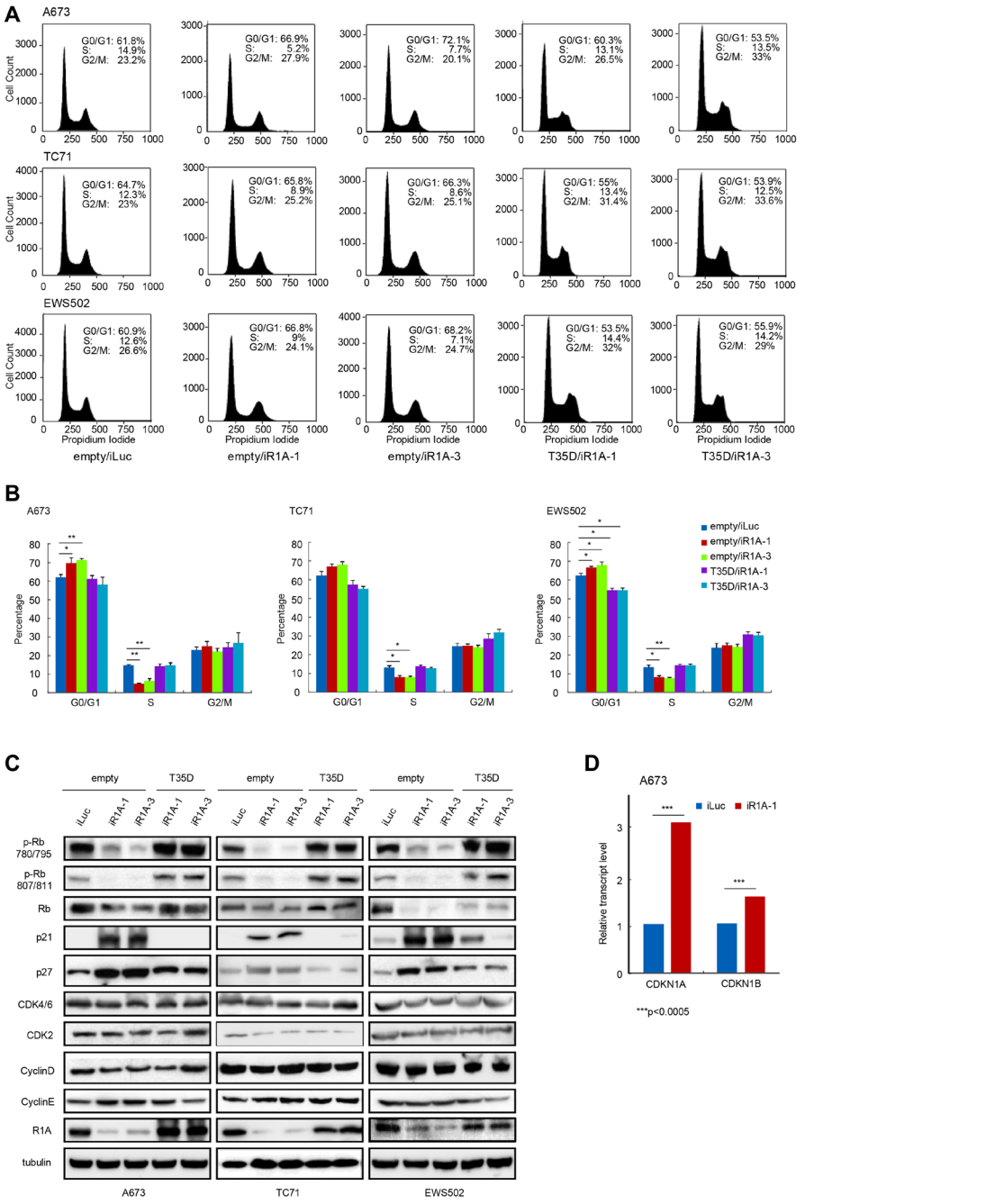

Figure 2: PPP1R1A controls G1 to S transition in ES cell cycle. (**A** and **B**) PPP1R1A depletion induces blockage of cell cycle at G1 to S transition phase which can be released by expression of T35D. ES A673, TC71, and EWS502 cells with control (iLuc) or PPP1R1A (iR1A-1 or -3) knockdown and rescued by empty or T35D were subject to cell cycle analyses by propidium iodide staining followed by flow cytometry. Quantification of percentage of cell population underwent each cell cycle phase is shown in B. (**C** and **D**) Low levels of PPP1R1A (empty/iR1A-1 or empty/iR1A-3) results in hypophosphorylation while high levels of PPP1R1A (empty/iLuc, T35D/iR1A-1, T35D/iR1A-3) induces hyperphosphorylation of Rb protein at sites 780/795 and 807/811. G1 cell cycle inhibitors $p21^{Cip1}$ and $p27^{Kip1}$ are downregulated by PPP1R1A at protein and transcript levels as evidenced by western blotting (C) and RNA-seq (D) analyses. The stripes over the images of A673 CDK2 and CyclinD in C are scratches on the X-ray film. *CDKN1A* and *CDKN1B* are genes encoding $p21^{Cip1}$ and $P27^{Kip1}$, respectively. ***multiple testing adjusted $p < 0.0005$.

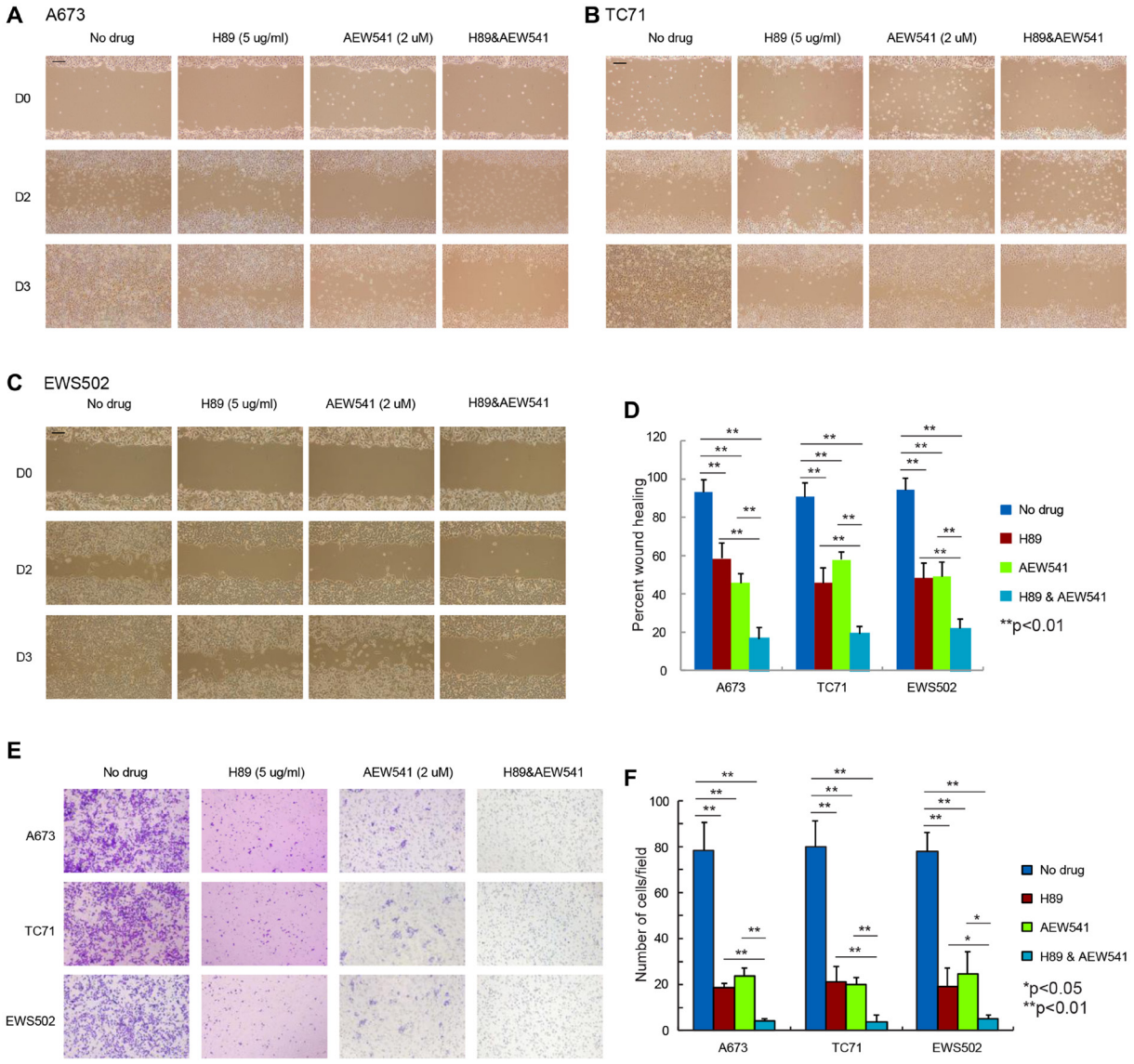

Figure 4: Simultaneous inhibition of PPP1R1A and IGF-1R pathways is more effective in limiting ES cell migration than single treatment. (**A**–**C**) A673 (A), TC71 (B), and EWS502 (C) ES cells treated with H89 in combination with AEW541 migrated much slower than the non-treated control or single agent treated cells. Scale bar equals 250 mm. (**D**) Quantification of wound healing assay results in three ES cell lines. $^{**}p < 0.001$. (**E**) Boyden chamber transwell assay results showing that ES cell migration was significantly decreased when cells were treated with H89 and AEW541 compared with cells treated with or without H89 or AEW541 alone. (**F**) Quantification of the number of migrated cells per field in transwell assay in E. $^{**}p < 0.01$, $^{*}p < 0.05$.

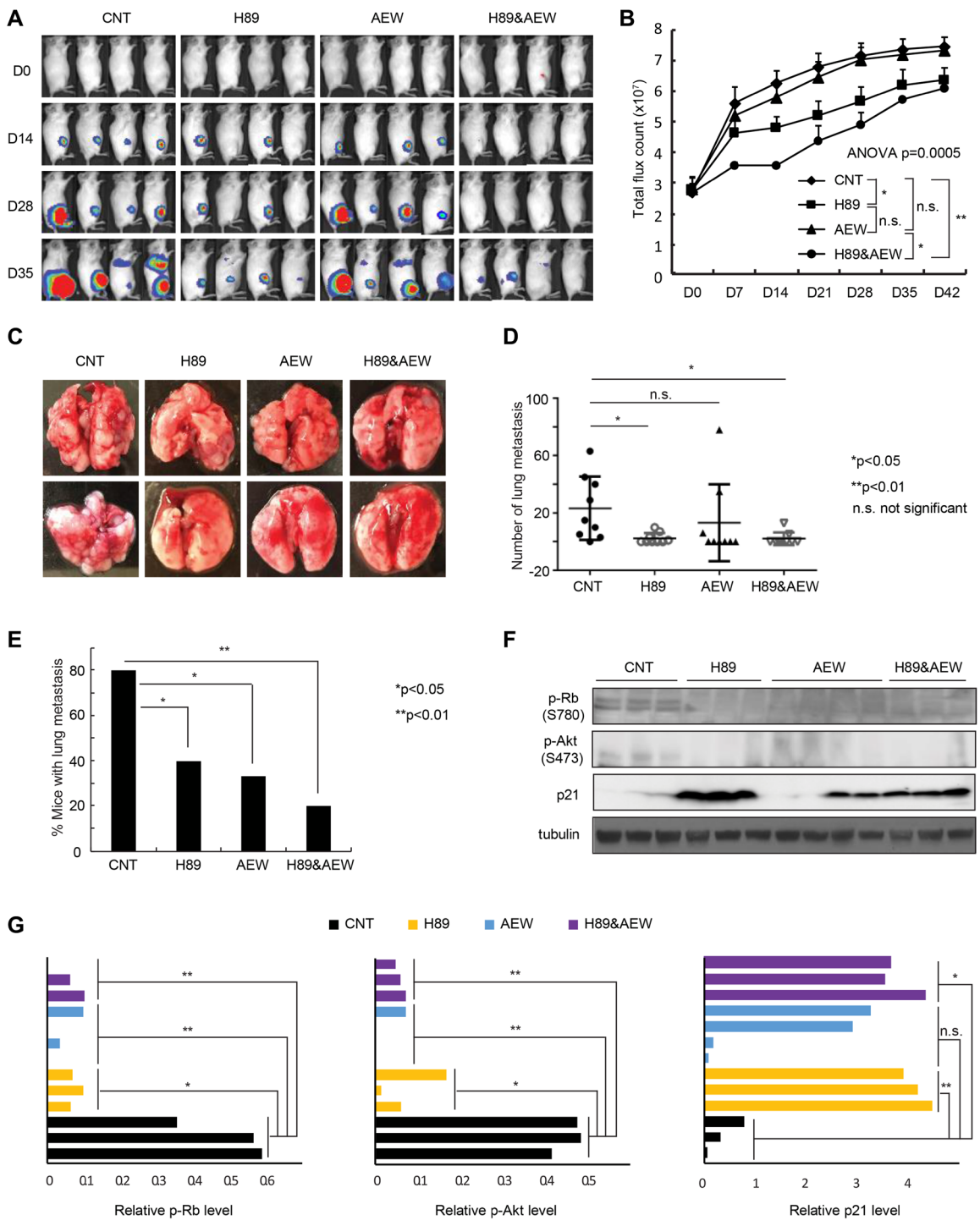

Figure 5: Combination of PPP1R1A and IGF-1R inhibition is more active in limiting ES tumor growth and metastasis than either individual treatment in an orthotopic xenograft mouse model. (**A**) and (**B**) *In vivo* xenograft studies measuring tumor growth in animals injected with luciferase expressing A673 cells and treated with vehicle or 8 mg/kg H89 or 50 mg/kg AEW541 or H89 together with AEW541 in intratibial injection mouse model. $n = 10$ for each group. ANOVA test $p = 0.0005$. *post hoc test $p < 0.05$; $^{**}p < 0.01$; n. s. not significant. (**C**) Representative images of lungs from the animals injected with A673 cells and treated with vehicle or H89 or AEW541 or H89 with AEW541 as indicated. (**D**) and (**E**) Graphs showing the number of metastatic nodules in each lung (D) and the percentage of mice with pulmonary lesions (E) in each indicated condition. *Student's *t*-test $p < 0.05$; n. s., not significant in (D). *Two samples *Z* test for proportions $p < 0.05$, $^{**}p < 0.01$ in (E). (**F**) and (**G**) p21^{Cip1} protein and phosphorylated Rb and Akt levels in tumors harvested from different treatment groups as indicated.